

Appendix

Posterior Epiphyseal Orientation of the Proximal Part of the Femur in Slipped Capital Femoral Epiphysis

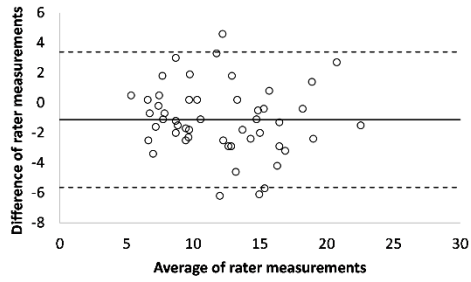
Several measurements have been described to evaluate the epiphyseal orientation in slipped capital femoral epiphysis (SCFE), including the Southwick angle²⁵, slipping angle¹⁹, posterior sloping angle^{10,14,15,18}, and epiphyseal tilt^{20,24}. All of these measurements are based on the epiphyseal plane, which is defined by a line connecting the epiphyseal edges (line “AB” in Fig. E-2). However, some variation can be found among the results of these measurements on the same radiograph.

The Southwick angle²⁵ is formed by a line perpendicular to the epiphyseal plane and the anatomical axis of the femoral diaphysis (Fig. E-2A). The Southwick angle may be influenced by femoral positioning and by retroversion of the femoral neck.

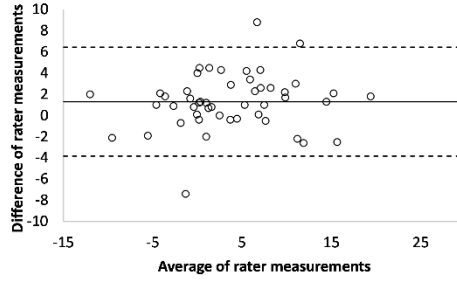
The slipping angle¹⁹ is the angle between the epiphyseal plane and a line (“S” in Fig. E-2B) perpendicular to the bisector line between the femoral neck and shaft axes. It was originally described for a specific lateral view of the proximal part of the femur, with 25° of flexion and 90° of external rotation, so this measurement may be not applicable to general lateral views.

The posterior sloping angle was originally measured using the epiphyseal line and a line perpendicular to the neck-shaft axis¹⁰. The neck-shaft axis is defined by a line connecting the middle points of the neck (“C” in Fig. E-2C) and shaft (“D” in Fig. E-2C) on Lauenstein radiographs made with 90° of hip flexion. There has been some criticism with regard to the level of the central point of the diaphysis when different degrees of hip flexion and rotation are observed on radiographs.

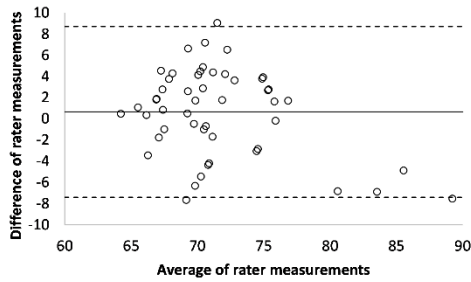
The posterior epiphyseal tilt angle is determined by a line perpendicular to the epiphyseal plane and the anatomical axis of the femoral neck^{20,24} (Fig. E-2D).



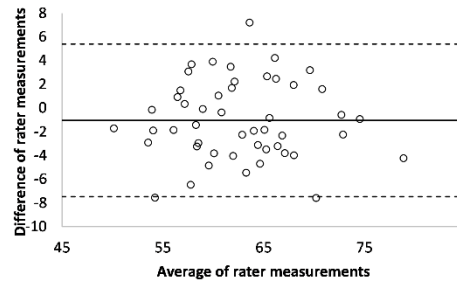
A. Frontal Tilt Angle



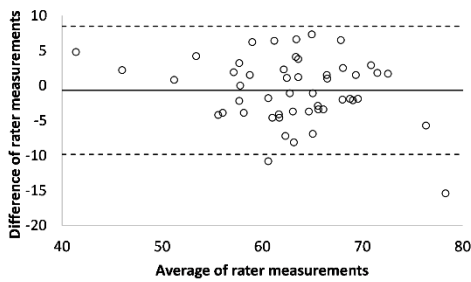
F. Lateral Tilt Angle



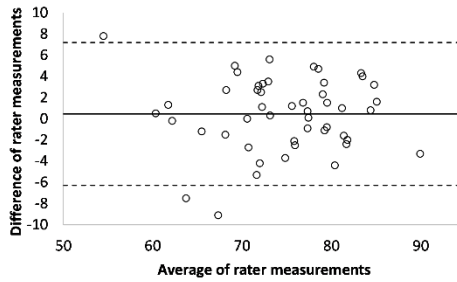
B. Superior Epiphyseal Extension Ratio



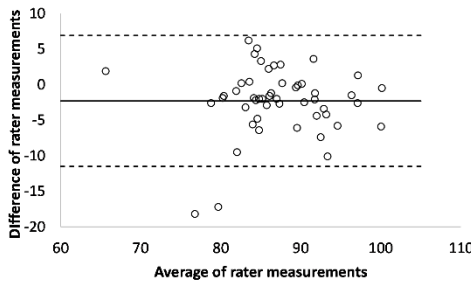
G. Anterior Epiphyseal Extension Ratio



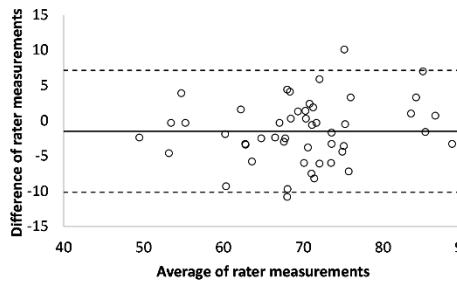
C. Superior Epiphyseal Angle



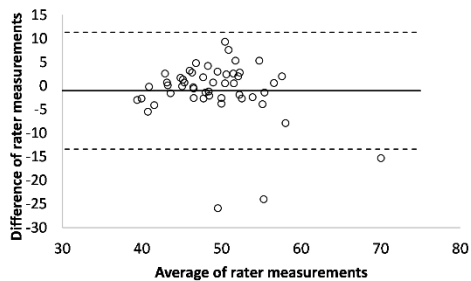
H. Anterior Epiphyseal Angle



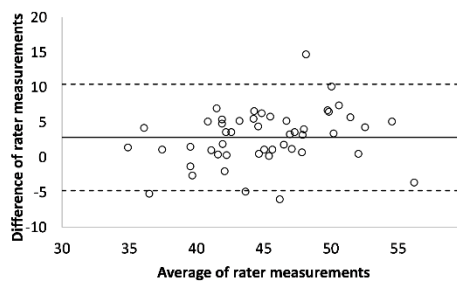
D. Inferior Epiphyseal Angle



I. Posterior Epiphyseal Angle



E. Superior Alpha Angle



J. Anterior Alpha Angle

Fig. E-1

Bland-Altman plots of the interrater reliability of the radiographic measurements on anteroposterior radiographs, including the frontal tilt angle (**Fig. E-1A**), superior epiphyseal extension ratio (**Fig. E-1B**), superior epiphyseal angle (**Fig. E-1C**), inferior epiphyseal angle (**Fig. E-1D**), and superior alpha angle (**Fig. E-1E**), and on frog-leg lateral radiographs, including the lateral tilt angle (**Fig. E-1F**), anterior epiphyseal extension ratio (**Fig. E-1G**), anterior epiphyseal angle (**Fig. E-1H**), posterior epiphyseal angle (**Fig. E-1I**), and anterior alpha angle (**Fig. E-1J**). The solid horizontal line represents the mean difference in measurements across raters, and the dashed lines represent the 95% limits of agreement.

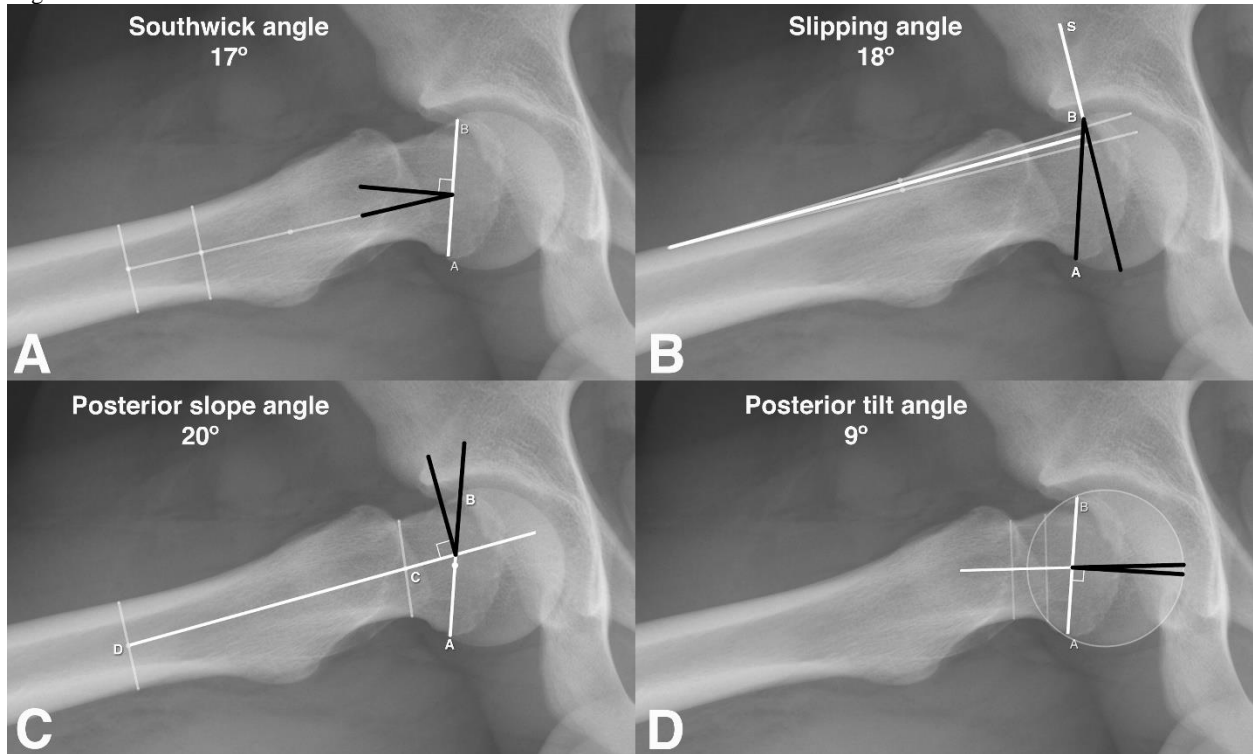


Fig. E-2

Lateral proximal femoral radiograph of a 16-year-old boy with left SCFE and no subsequent contralateral right hip slip after 18 months and achievement of skeletal maturity. Measurements to evaluate posterior epiphyseal inclination include the Southwick angle (**Fig. E-2A**), slipping angle (**Fig. E-2B**), posterior slope angle (**Fig. E-2C**), and posterior epiphyseal tilt angle (**Fig. E-2D**).